Synthetic Routes to Homoleptic Near-linear Mg and Ca Bulky Bis(silyl)amide Complexes

Ji-Dong Leng,[a,b] Conrad A. P. Goodwin,[b] Iñigo. J. Vitorica-Yrezabal,[b] and David P. Mills*[b]

[a.] Guangzhou Key Laboratory for Environmentally Functional Materials and Technology, School of Chemistry and Chemical Engineering, Guangzhou University, 230 Wai Huan Xi Road, Guangzhou Higher Education Mega Center, Guangzhou, 510006, P. R. China.

[b.] School of Chemistry, The University of Manchester, Oxford Road, Manchester, M13 9PL, UK.

Contents

1. NMR spectroscopic data for 1-4 and 6

Figure S1. ^{1}H NMR spectrum of **1** in d_6-benzene/THF.
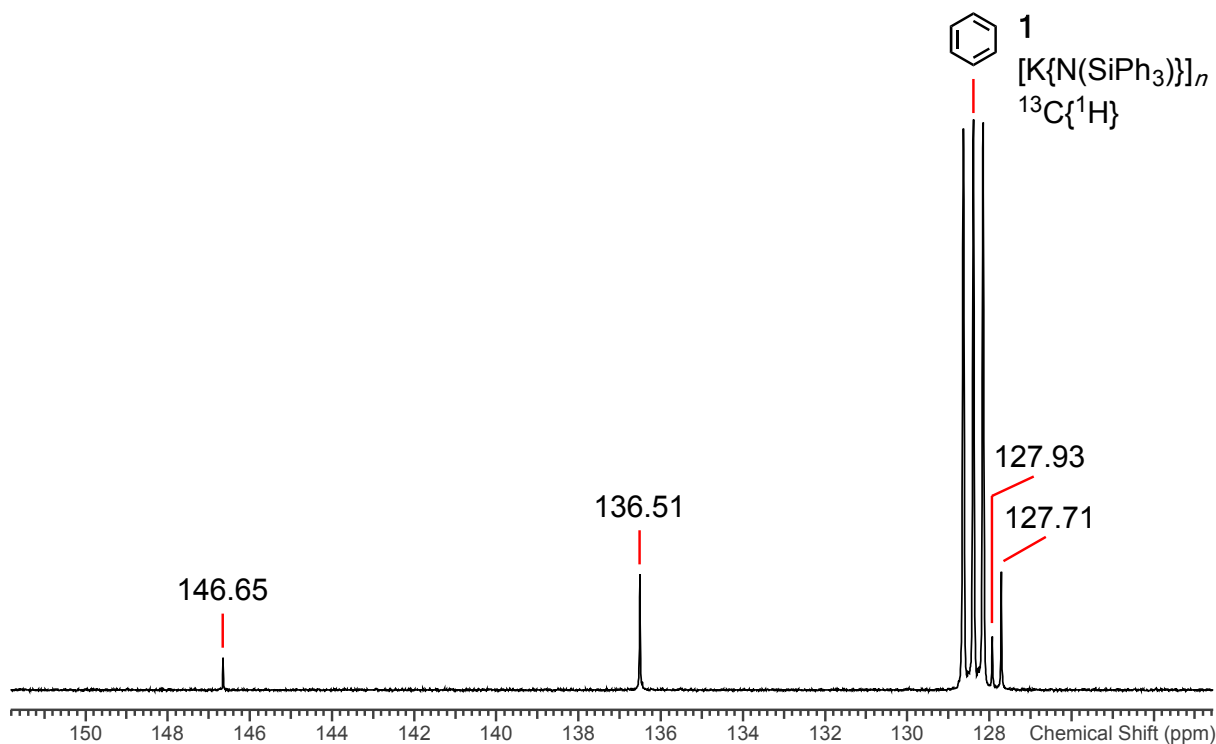
**Figure S2**. ^{13}C{^{1}H} NMR spectrum of **1** in d_6-benzene/THF.
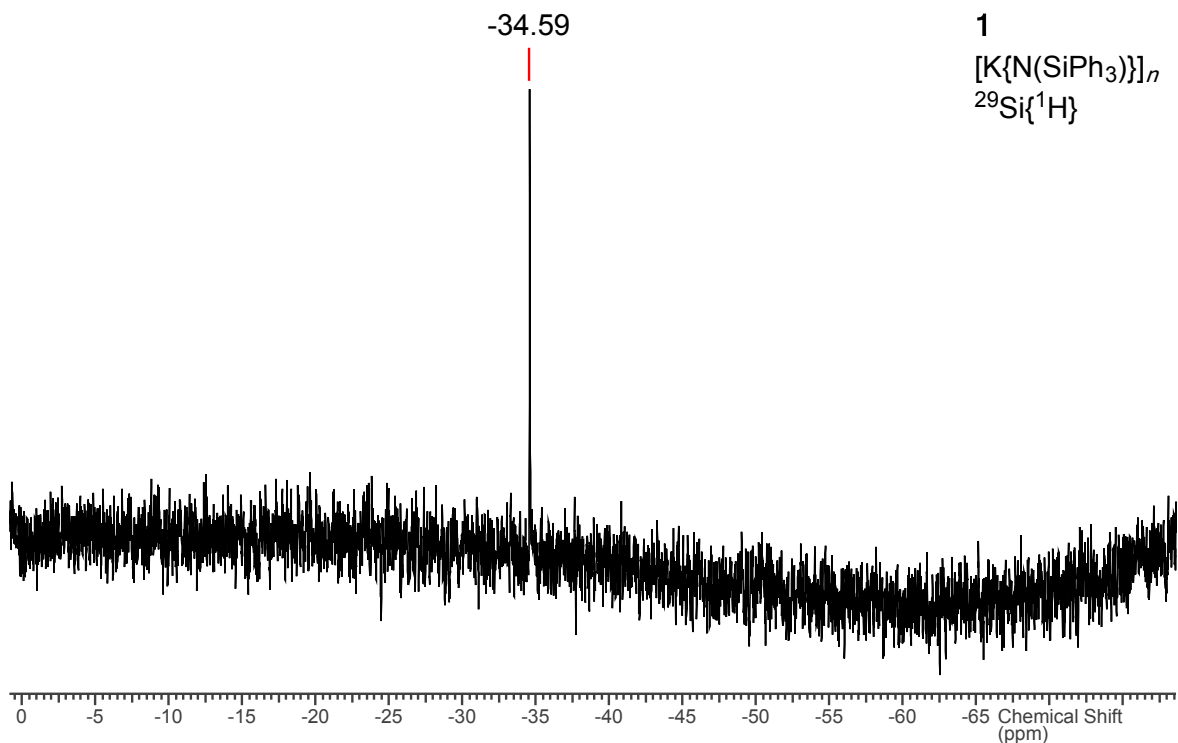
Figure S3. $^{29}Si\{^1H\}$ NMR spectrum of **1** in d_6-benzene/THF.
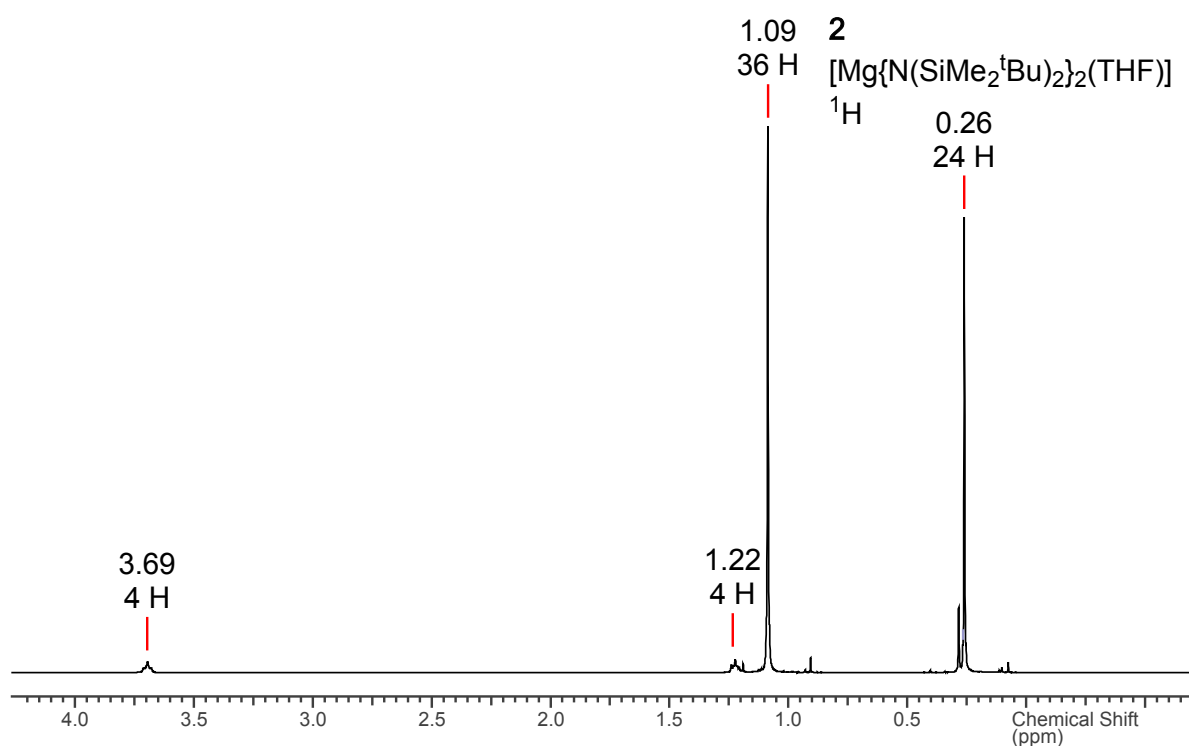
Figure S4. ^1H NMR spectrum of **2** in d_6-benzene.
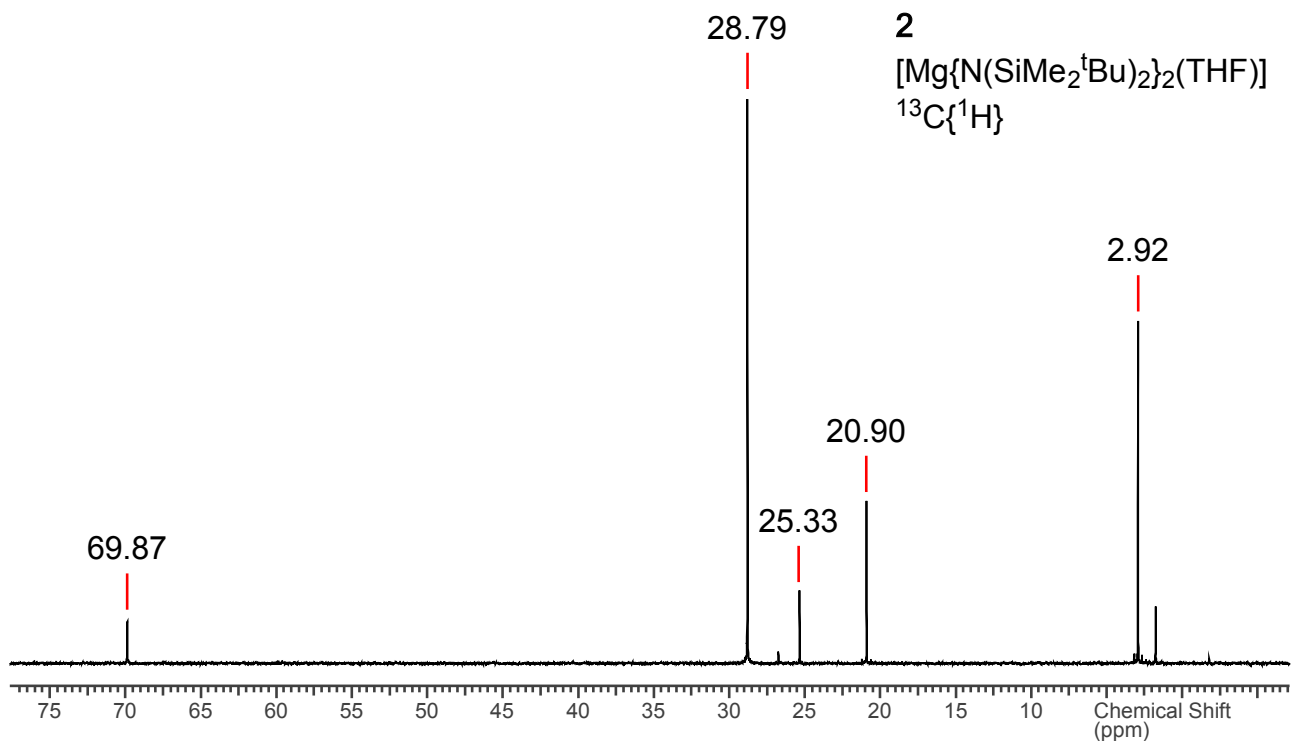
Figure S5. $^{13}C\{^1H\}$ NMR spectrum of **2** in d_6-benzene.
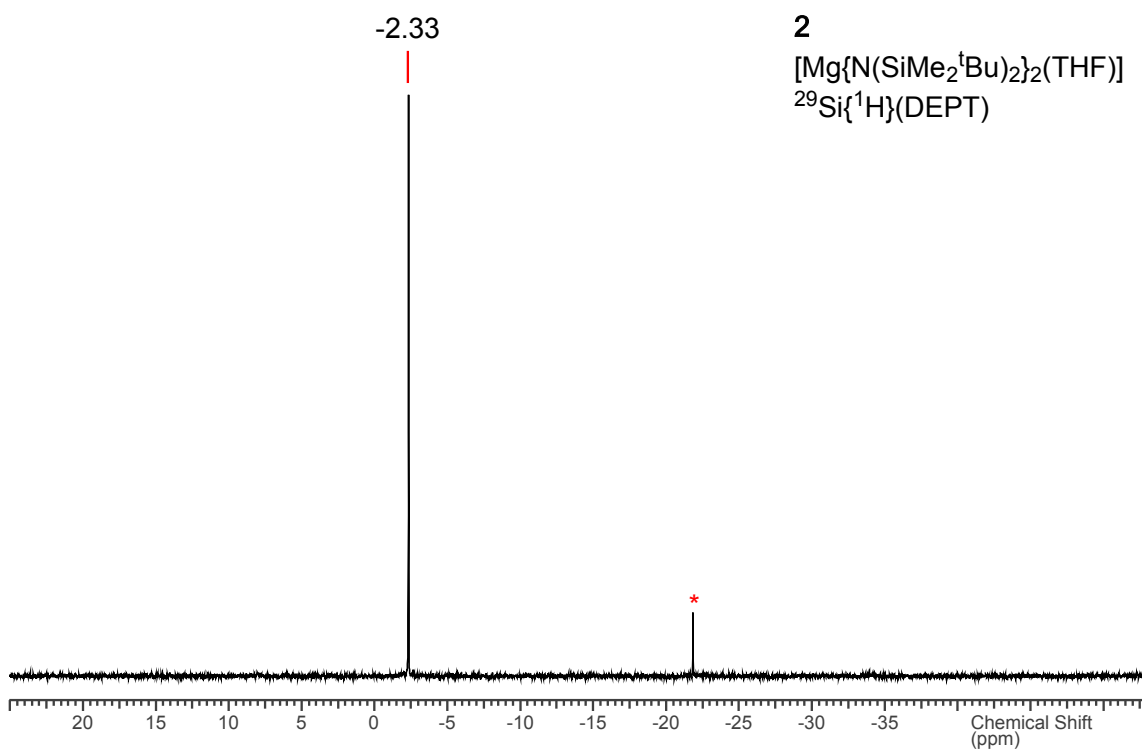
Figure S6. $^{29}Si\{^1H\}$(DEPT) NMR spectrum of **2** in d_6-benzene. * denotes a silicone grease impurity.
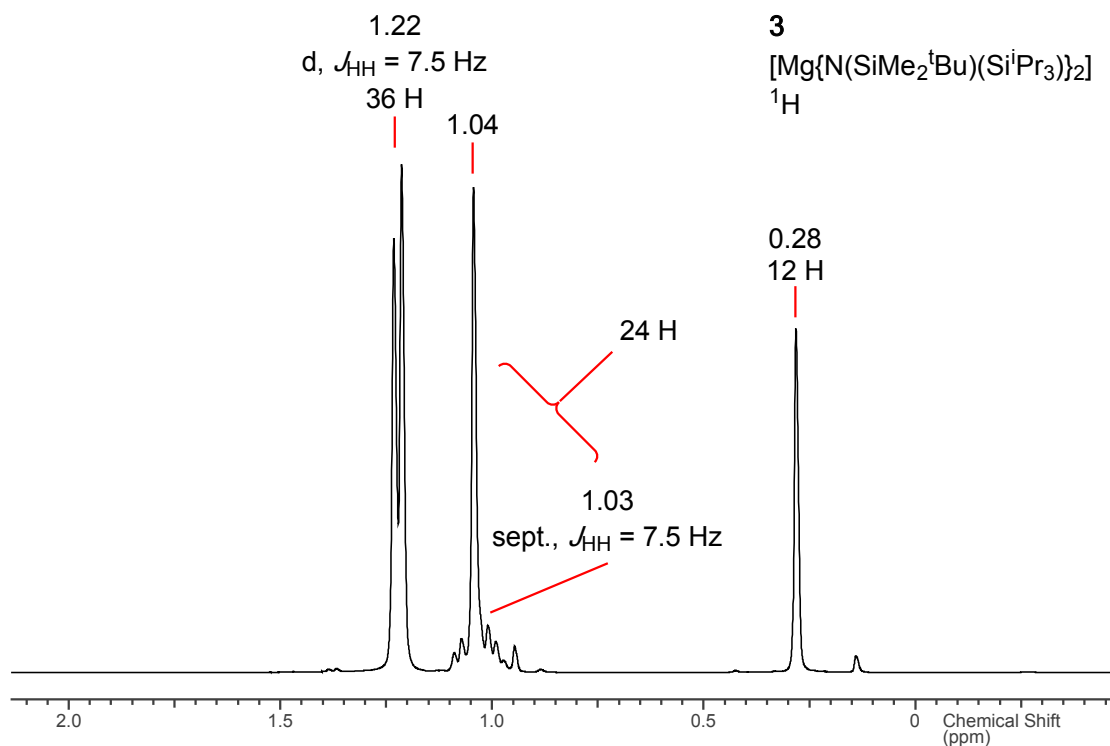
Figure S7. ^{1}H NMR spectrum of **3** in d_6-benzene.
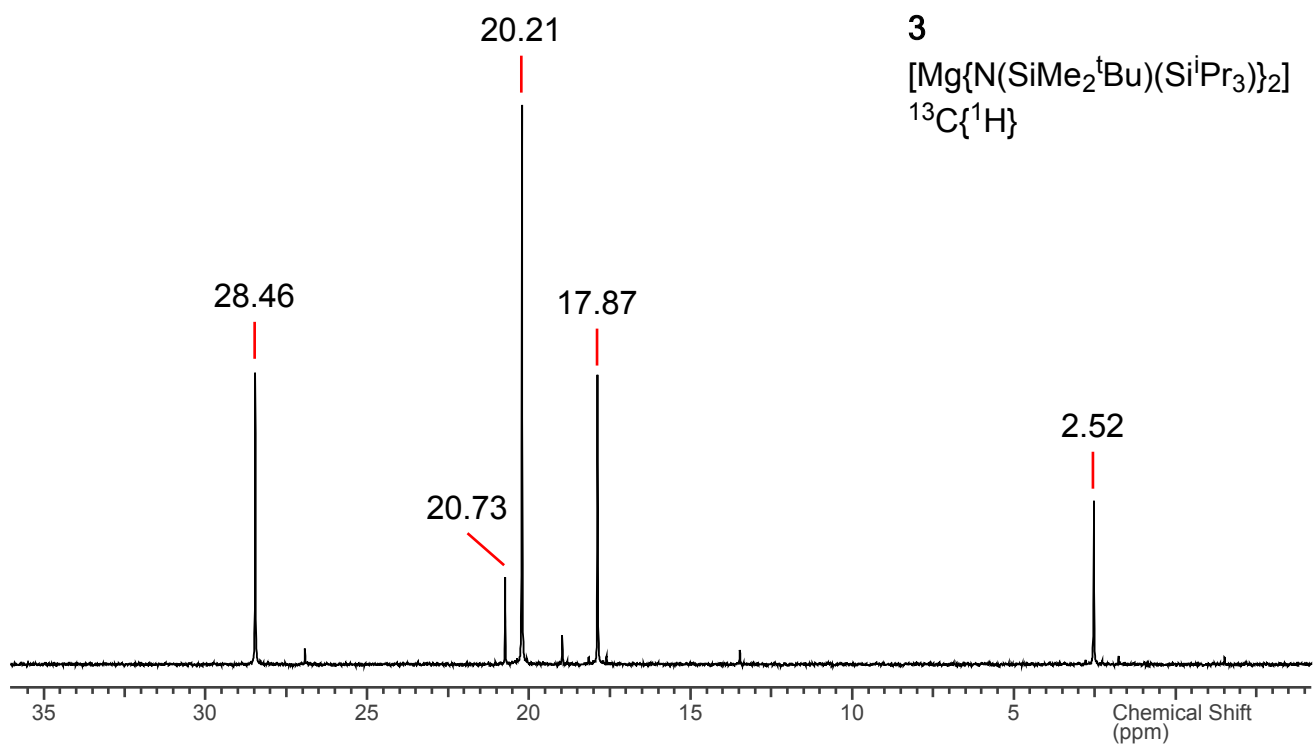
Figure S8. ^{13}C{^{1}H} NMR spectrum of **3** in d_6-benzene.
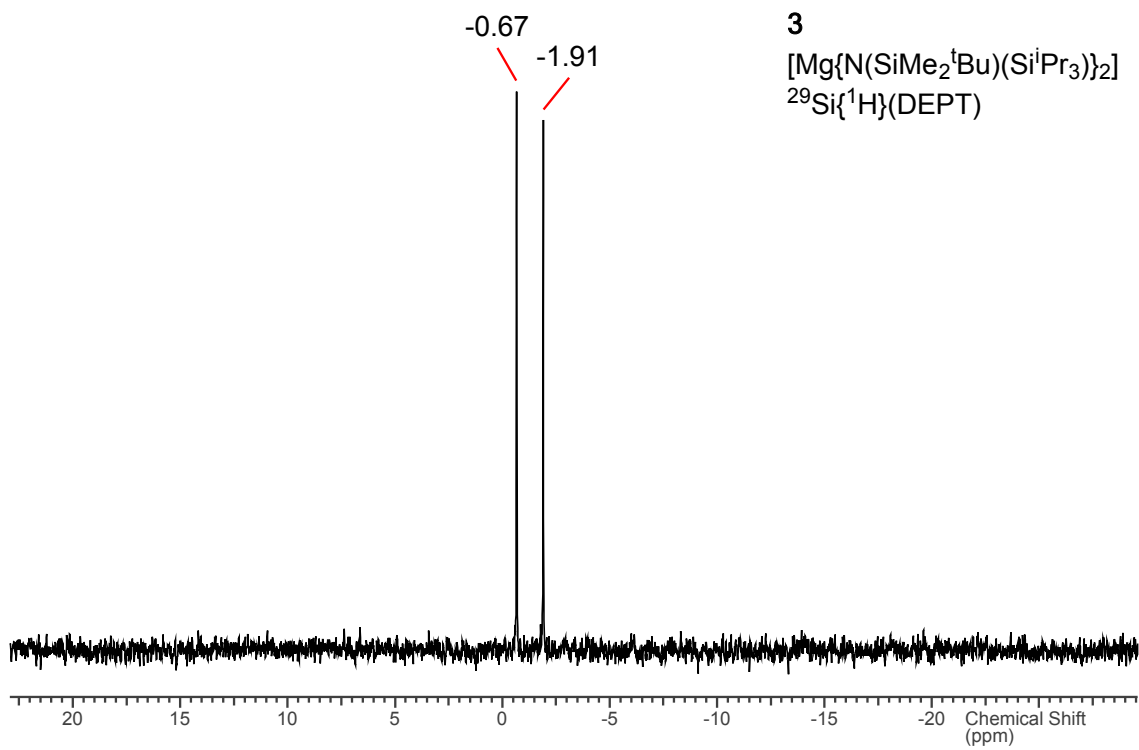
Figure S9. $^{29}Si\{^1H\}$(DEPT) NMR spectrum of **3** in d_6-benzene.

-0.67

-1.91

3

[Mg{N(SiMe$_2$^tBu)(Si^iPr$_3$)}$_2$]

$^{29}Si\{^1H\}$(DEPT)
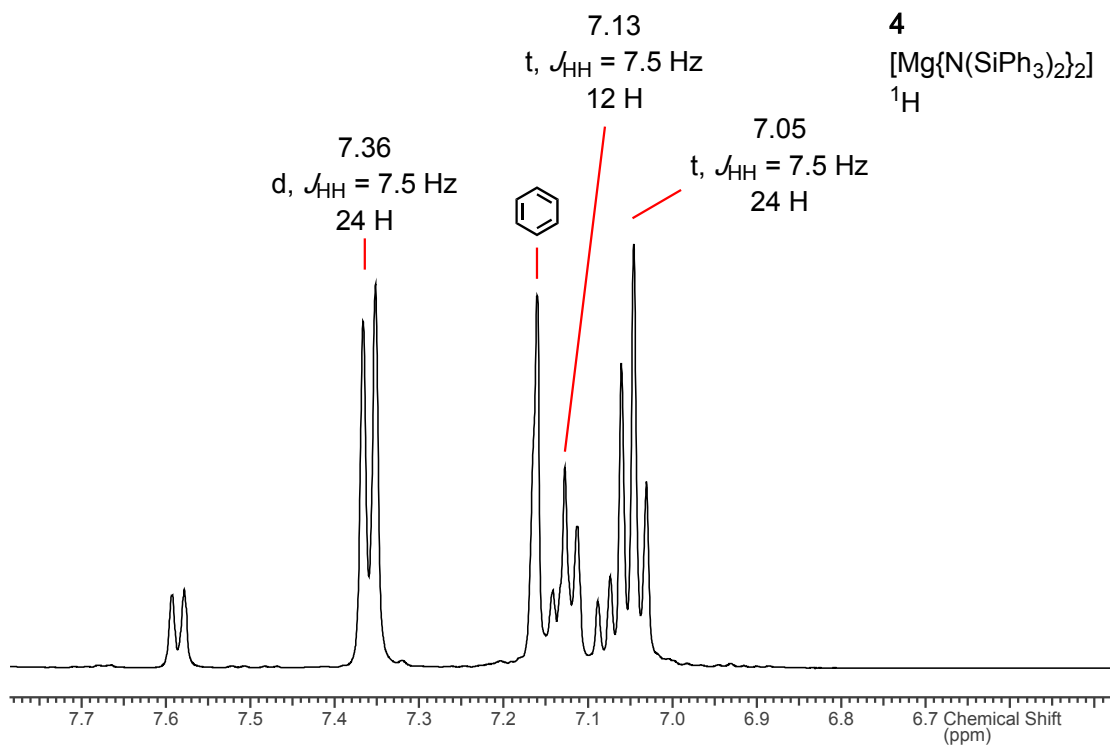
Figure S10. ^1H NMR spectrum of **4** in d_6-benzene.

7.13

t, J_{HH} = 7.5 Hz

12 H

7.05

t, J_{HH} = 7.5 Hz

24 H

7.36

d, J_{HH} = 7.5 Hz

24 H

4

[Mg{N(SiPh$_3$)$_2$}$_2$]

^1H
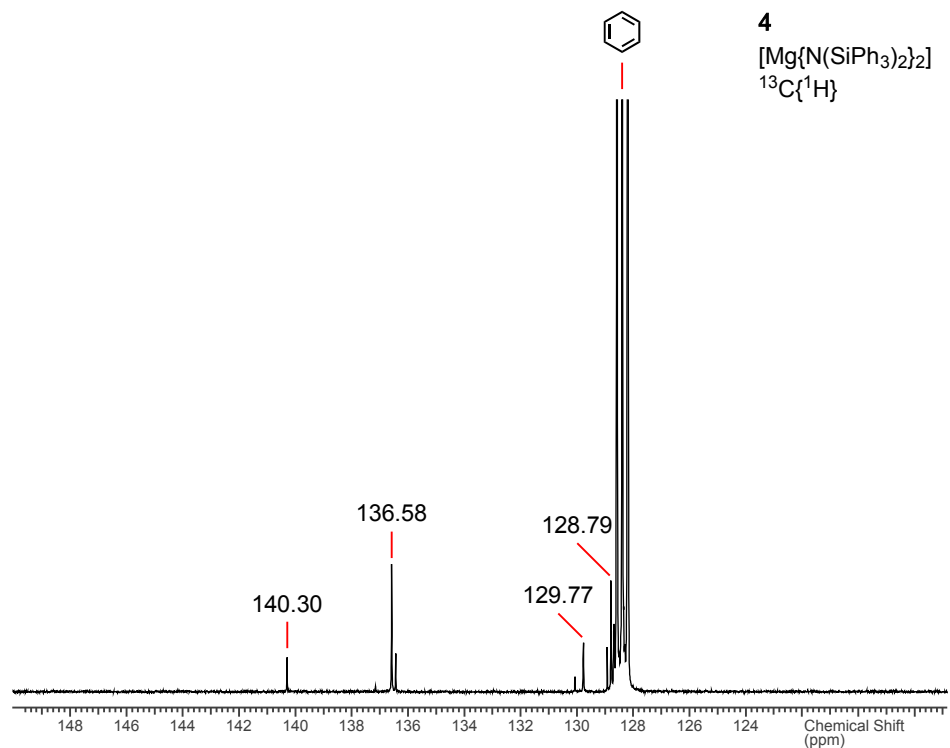
Figure S11. $^{13}C\{^1H\}$ NMR spectrum of **4** in d_6-benzene.
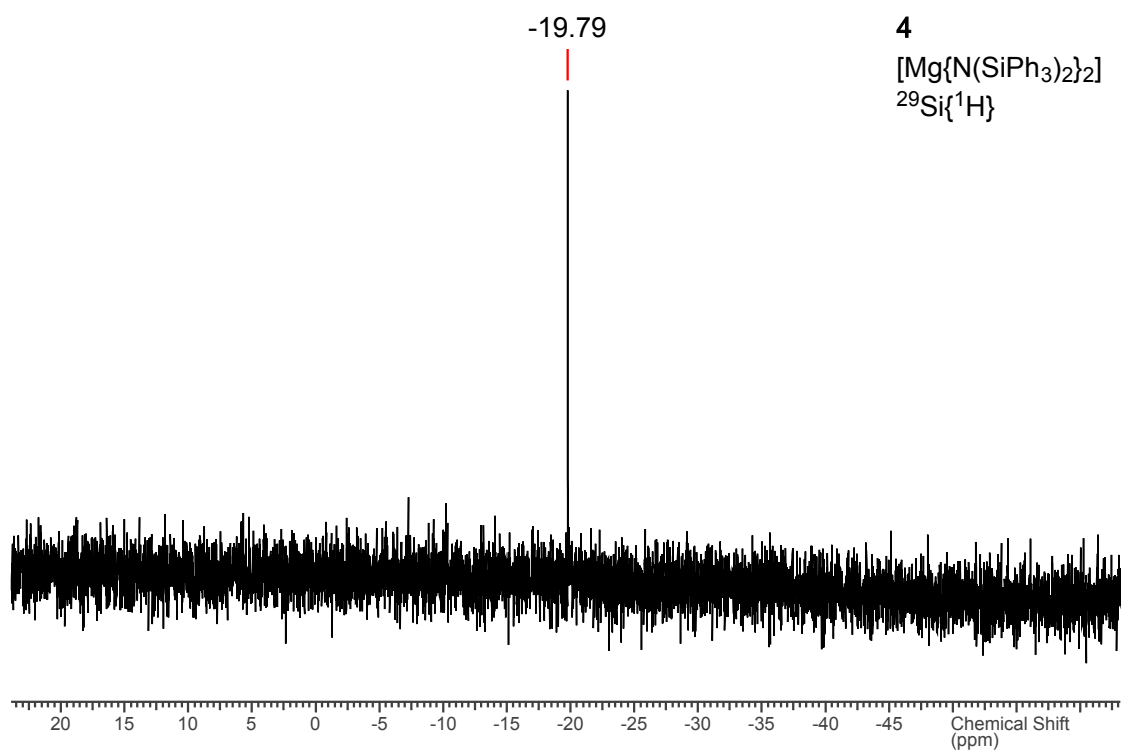
Figure S12. $^{29}Si\{^1H\}$ NMR spectrum of **4** in d_6-benzene.
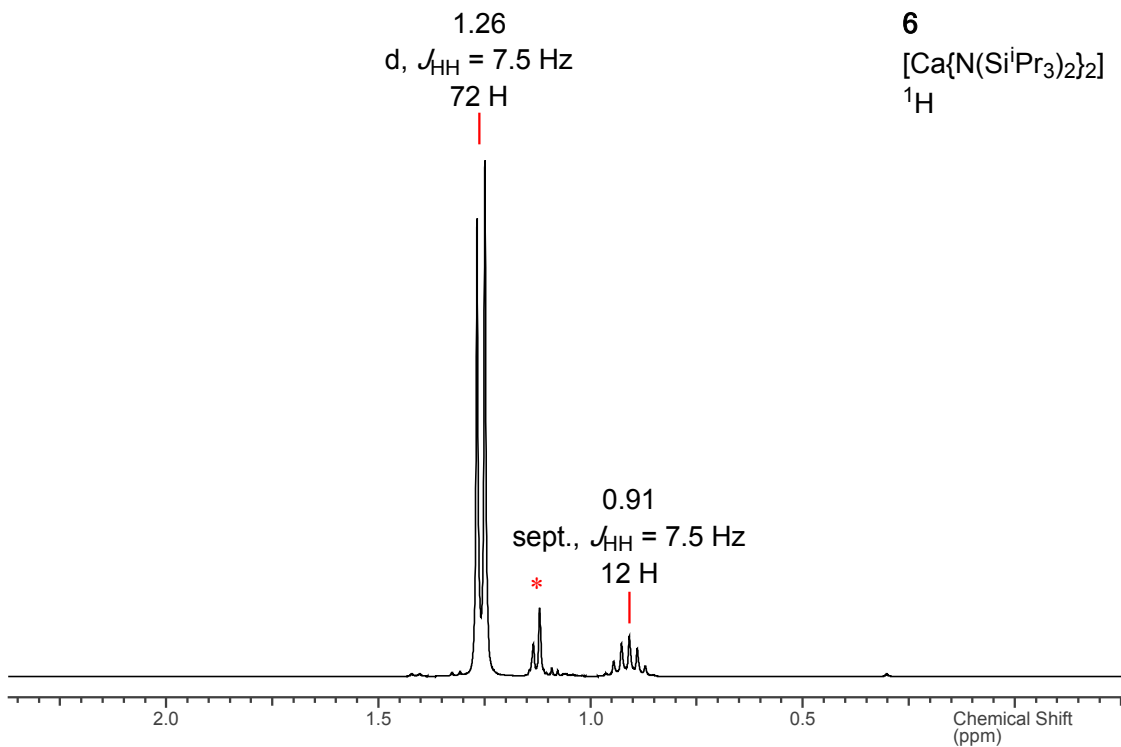
Figure S13. ^{1}H NMR spectrum of **6** in d_6-benzene. * denotes HN(Si^{i}Pr$_3$)$_2$ impurity.
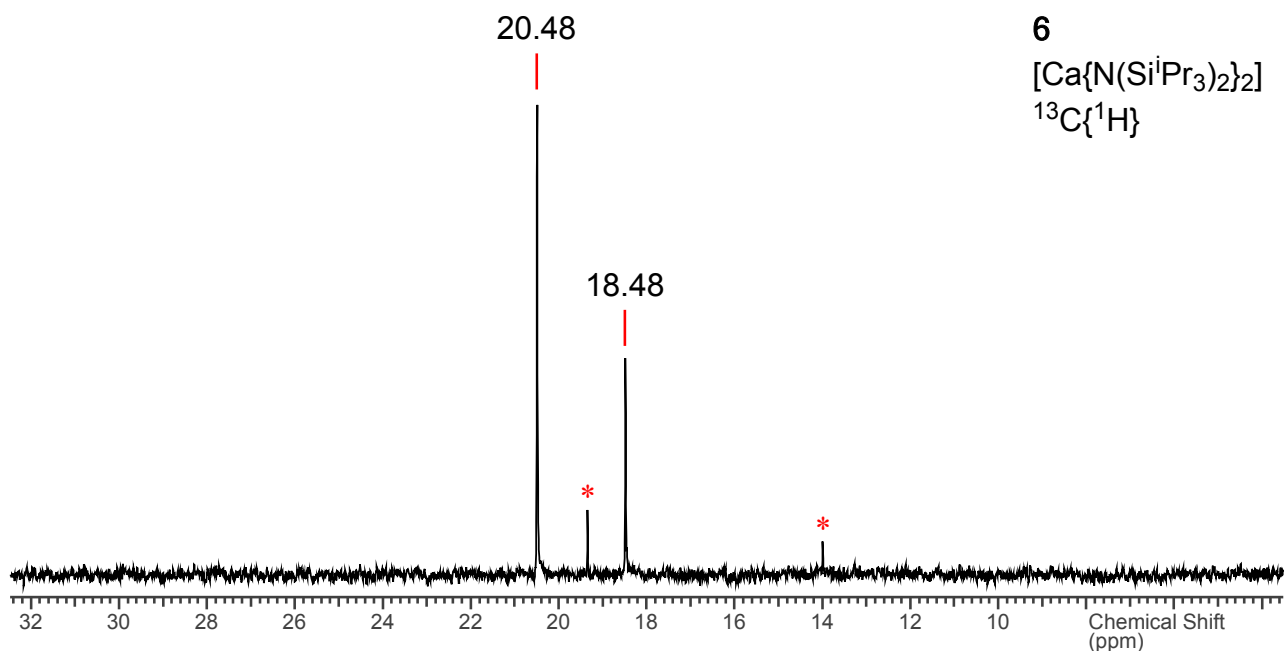
Figure S14. ^{13}C{^{1}H} NMR spectrum of **6** in d_6-benzene. * denotes HN(Si^{i}Pr$_3$)$_2$ impurity.
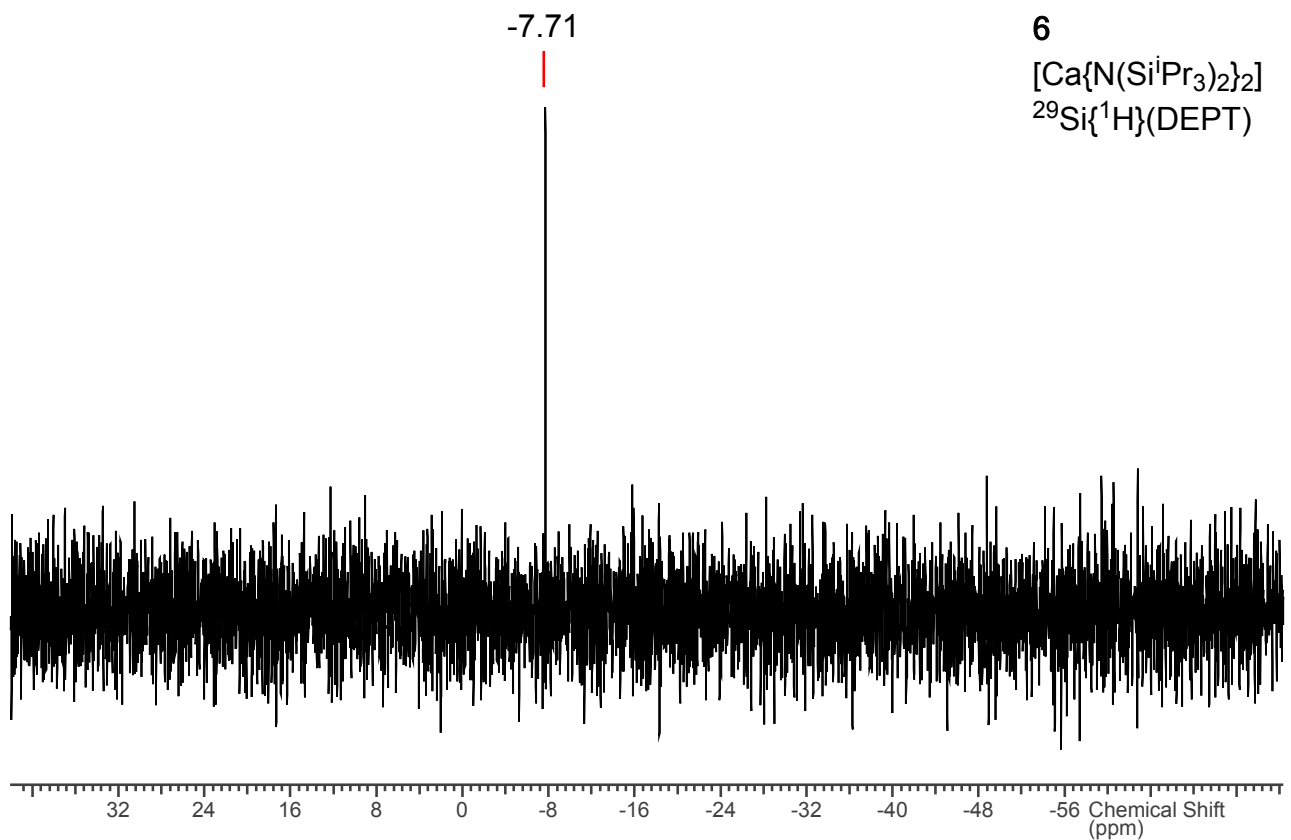
Figure S15. $^{29}Si\{^{1}H\}$(DEPT) NMR spectrum of **6** in d_6-benzene.

2. DOSY NMR spectroscope data for 2-4 and 6.

[1]H DOSY measurements were carried out non-spinning at 295 K on a Bruker Avance III+ spectrometer operating at 500.19 MHz with a Prodigy cryoprobe, using the standard ledbpgp2s pulse sequence. Data were acquired with an array of 16 gradient amplitudes in equal steps of gradient squared, using 32 768 complex data points.
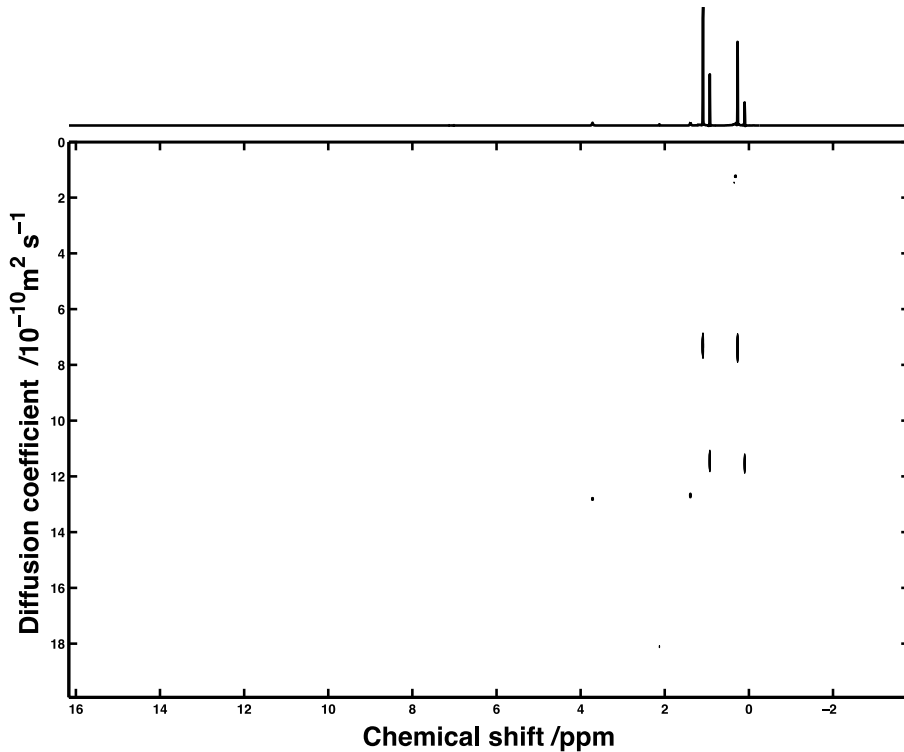
Figure S16. DOSY NMR spectrum of **2** recorded at 298 K in d_8-toluene.
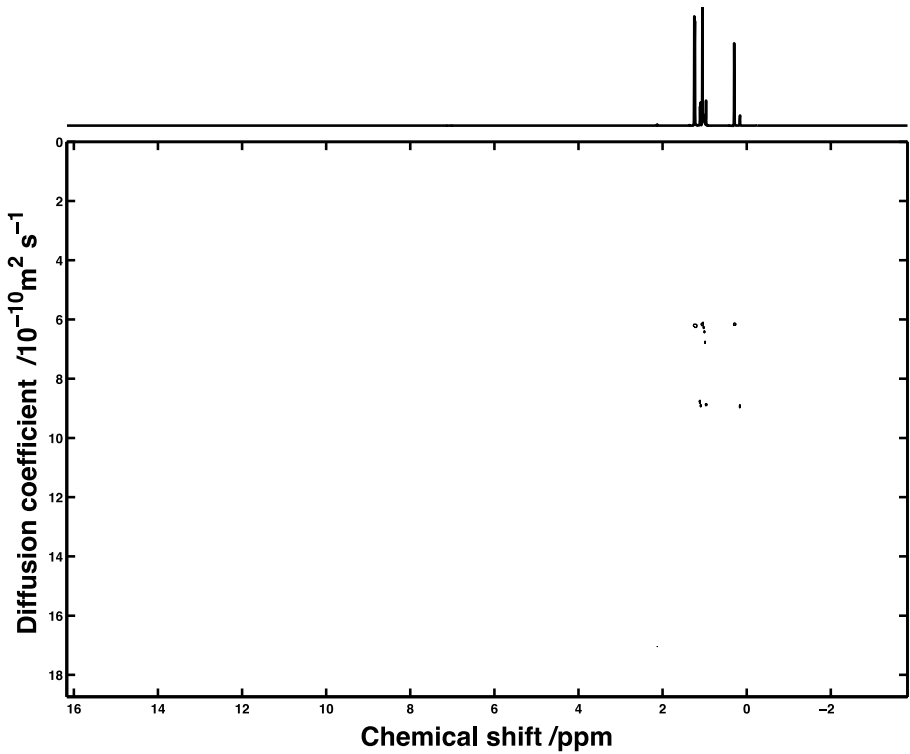
Figure S17. DOSY NMR spectrum of **3** recorded at 298 K in d_8-toluene.
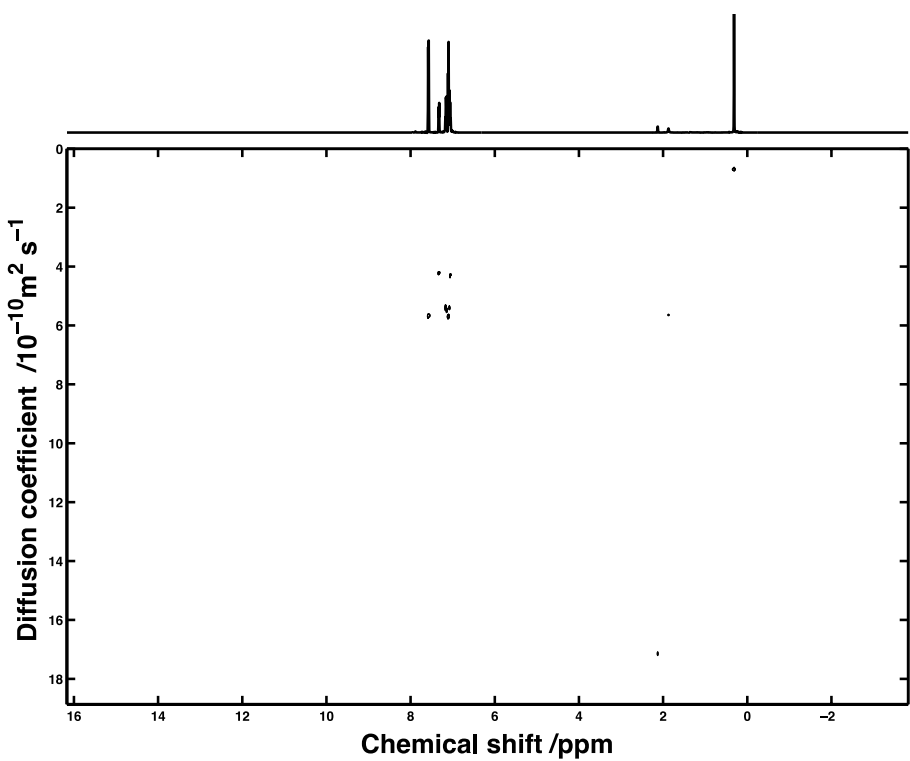
Figure S18. DOSY NMR spectrum of **4** recorded at 298 K in d_8-toluene.
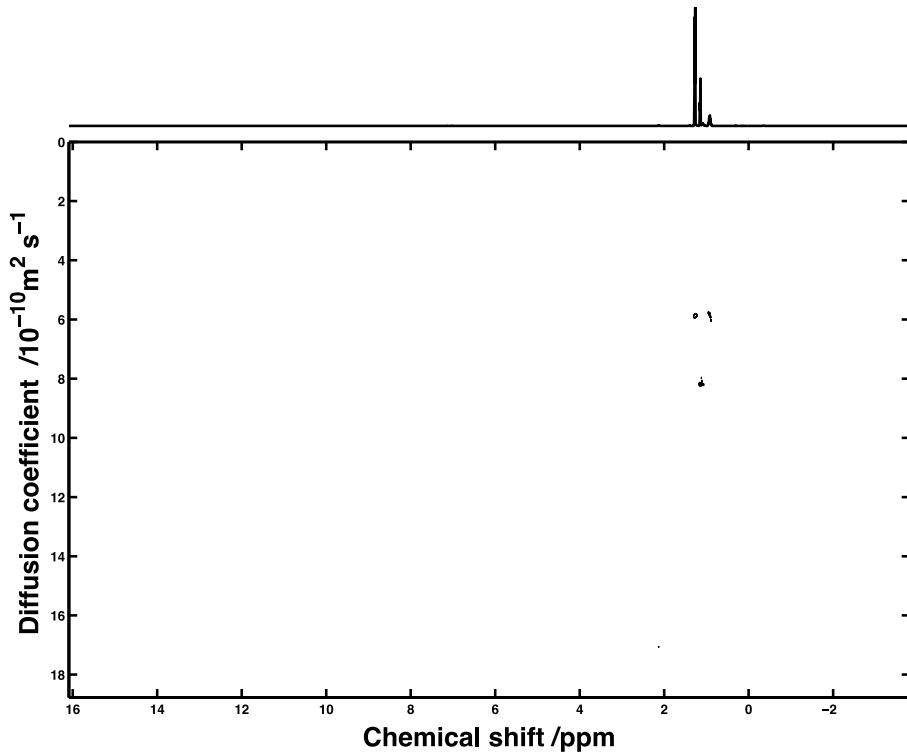
Figure S19. DOSY NMR spectrum of **6** recorded at 298 K in d_8-toluene.

Table S1. Processed DOSY NMR[1] data for **2**. Relevant peak information is highlighted in green.

Complex 2		Mw =	585.497			Type of Calculation	Mw --> D
Frequency	Exp. Ampl.	Fit Ampl1	Error	Diff. coef1	Error	D =	7.42
0.26713	0.70428	0.81689	0.01426	7.393	0.18912		
0.9646	0.00389	0.00444	0.00007	6.30045	0.1448		
1.05064	0.00584	0.00663	0.00015	7.01678	0.22774	Type of Calculation	D --> Mw
1.07322	0.01065	0.01262	0.00028	5.83661	0.19044	FW =	705.4
1.0903	1.00000	1.16292	0.01708	7.30946	0.15722		

		Average =	6.77126	0.41181
		D =	6.8(4)	

The above calculations are comparing calculated values for D and the molecular weight.

**Table S2.** Processed DOSY NMR data for **3**. Relevant peak information is highlighted in green.

Complex 3		Mw =	597.55			Type of Calculation	Mw --> D
Frequency	Exp. Ampl.	Fit Ampl1	Error	Diff. coef1	Error	D =	7.35
0.9945	0.02687	0.03117	0.00005	6.77288	0.01713		
1.00915	0.06669	0.07684	0.00008	6.41541	0.0098		
1.0244	0.09428	0.10843	0.00007	6.27922	0.00552	Type of Calculation	D --> Mw
1.03905	0.08767	0.10034	0.00015	6.14343	0.01378	Mw =	816.0
1.05552	0.92452	1.06139	0.00075	6.16476	0.00636		

		Average =	6.35514	0.02550
		D =	6.36(2)	

The above calculations are comparing calculated values for D and the molecular weight.

Table S3. Processed DOSY NMR data for **4**. Relevant peak information is highlighted in green or orange.

Complex 4		Mw =	1089.905			Type of Calculation	Mw --> D
Frequency	Exp. Ampl.	Fit Ampl1	Error	Diff. coef1	Error	D =	5.58
7.03007	0.01437	0.01569	0.00008	4.1792	0.03027		
7.04715	0.12256	0.13449	0.00016	4.27544	0.00723		
7.06241	0.26501	0.28955	0.00094	4.31698	0.02038	Type of Calculation	D --> Mw
7.08132	0.37437	0.4203	0.00109	5.40503	0.02039	Mw =	1278.2
7.09719	0.78215	0.88461	0.0019	5.69301	0.01787		
7.11183	0.52159	0.58987	0.00143	5.70556	0.02011		
7.14601	0.30172	0.33893	0.0011	5.48332	0.02606	Type of Calculation	D --> Mw
7.16004	0.34819	0.39054	0.00115	5.37904	0.02303	Mw =	2217.4
7.17408	0.13219	0.14732	0.00098	5.39969	0.05246		
7.56949	0.78594	0.8894	0.00142	5.66616	0.01323		
7.58414	0.748	0.84565	0.00197	5.68749	0.01928	The above calculations are comparing calculated values for D and the molecular weight.	
7.64089	0.00713	0.00772	0.00008	3.96315	0.05803		
7.65431	0.00718	0.00775	0.00006	3.96636	0.04222		
7.67262	0.00433	0.00469	0.00008	4.72853	0.11893	2 difference diffusion coefficients were	
7.68726	0.00435	0.00468	0.00008	4.70182	0.11865	observed for **4**, giving two separate Mw	
7.72509	0.00604	0.00658	0.00009	4.77231	0.09176	estimations, with one being	
7.73913	0.00589	0.00639	0.00011	4.66146	0.11681	approximately double the other.	
7.8807	0.00824	0.00911	0.00008	4.8169	0.06021		
7.88802	0.00894	0.00976	0.00009	4.77208	0.06334		
		Average =		5.20517	0.25213		
		D =		5.2(3)			
		Average =		4.14023	0.10809		
		D =		4.1(1)			

Table S4. Processed DOSY NMR data for **6**. Relevant peak information is highlighted in green.

Complex 6		Mw =	697.482			Type of Calculation	Mw --> D
Frequency	Exp. Ampl.	Fit Ampl1	Error	Diff. coef1	Error	D =	6.84
0.87612	0.00344	0.00396	0.00003	6.14608	0.06948		
0.89016	0.02208	0.02531	0.00005	6.02725	0.0163		
0.9048	0.06338	0.0724	0.00006	5.9092	0.00751	Type of Calculation	D --> Mw
0.92006	0.09275	0.10585	0.00015	5.83185	0.0119	Mw =	1000.0
0.9347	0.0754	0.08587	0.00007	5.8123	0.007		
0.94935	0.03147	0.03584	0.00005	5.77829	0.01218	The above calculations are comparing	
0.96399	0.00575	0.00655	0.00002	5.7798	0.02325	calculated values for D and the molecular	
1.1977	0.00176	0.00196	0.00001	5.32387	0.04779	weight.	
1.21357	0.00242	0.00271	0.00002	5.59397	0.05873		
1.26482	0.9917	1.13259	0.00154	5.87209	0.01168		
1.27947	0.90716	1.03642	0.00149	5.88697	0.01237		
1.38748	0.00502	0.00571	0.00001	5.91839	0.02246		
1.40212	0.00465	0.00528	0.00001	5.8786	0.02012		
		Average =		5.82759	0.11385		
		D =		5.8(1)			

## 3. FTIR spectroscopic data for 1-4 and 6
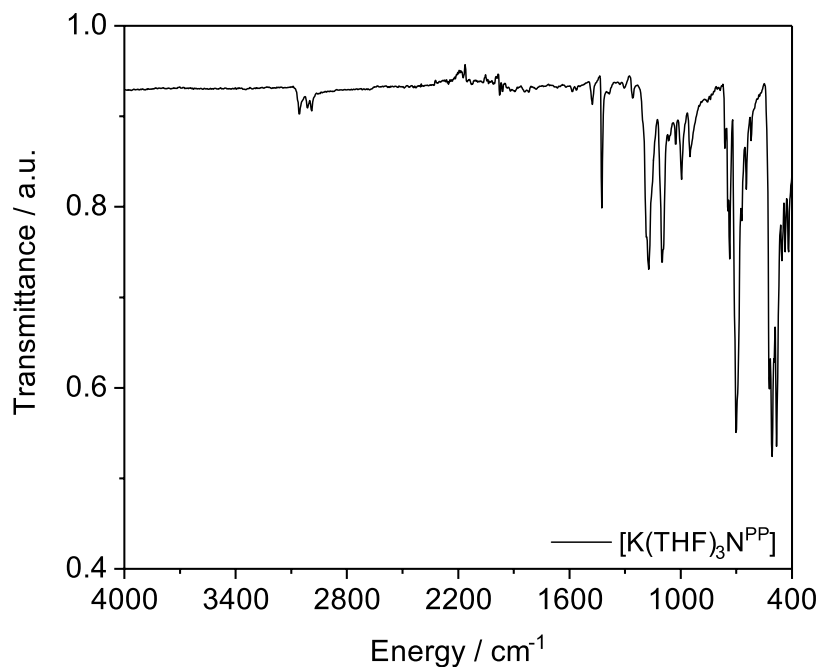
**Figure S20**. FTIR spectrum of **1-THF** (ATR-IR, microcrystalline powder).
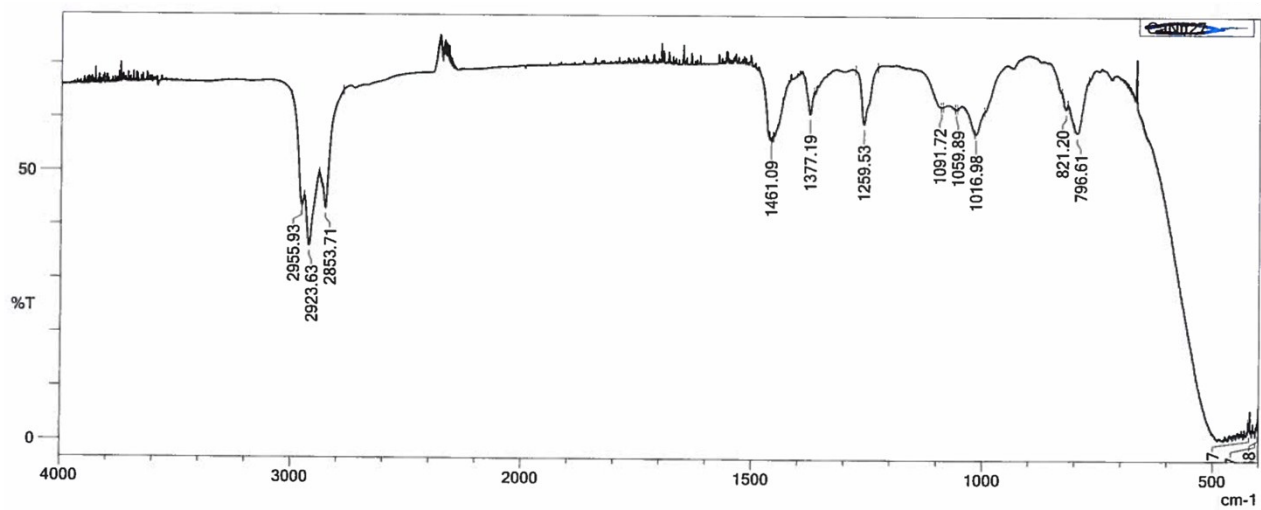
**Figure S21**. FTIR spectrum of **2** (Nujol mull, KBr discs).
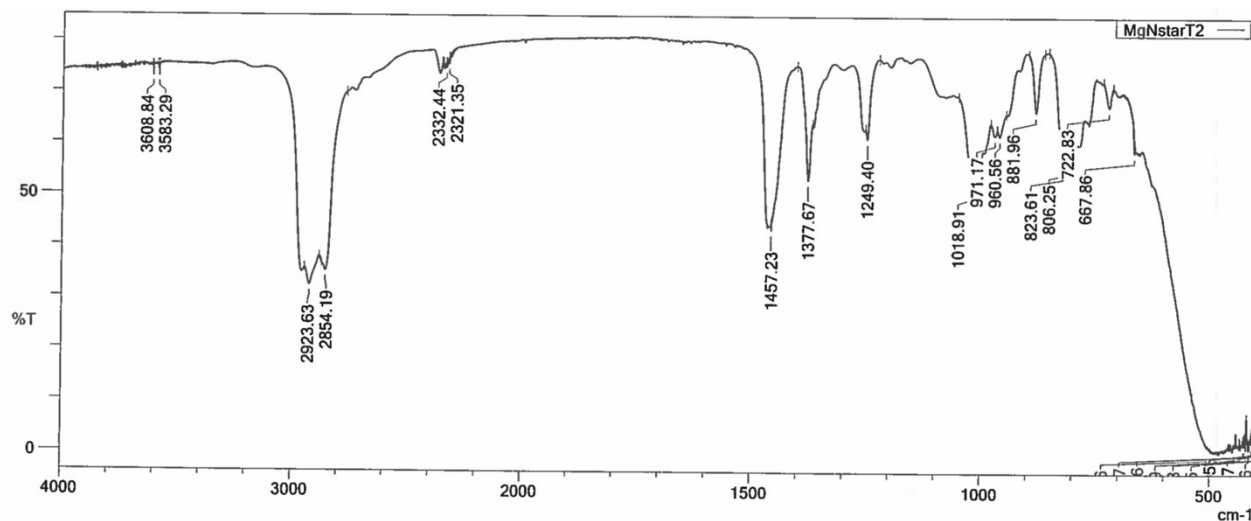
**Figure S22**. FTIR spectrum of **3** (Nujol mull, KBr discs).
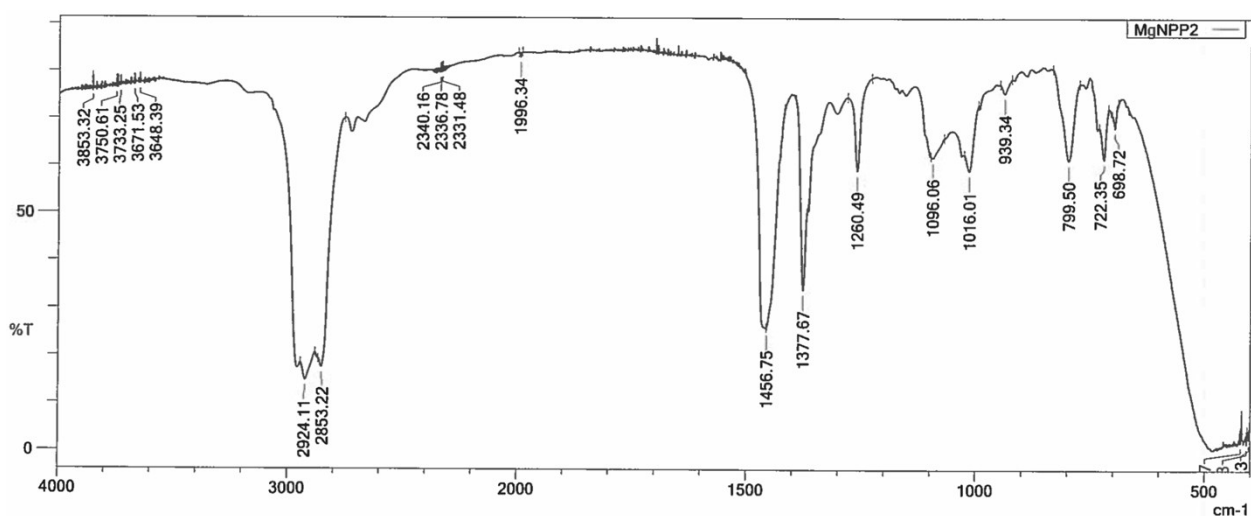
**Figure S23**. FTIR spectrum of **4** (Nujol mull, KBr discs).
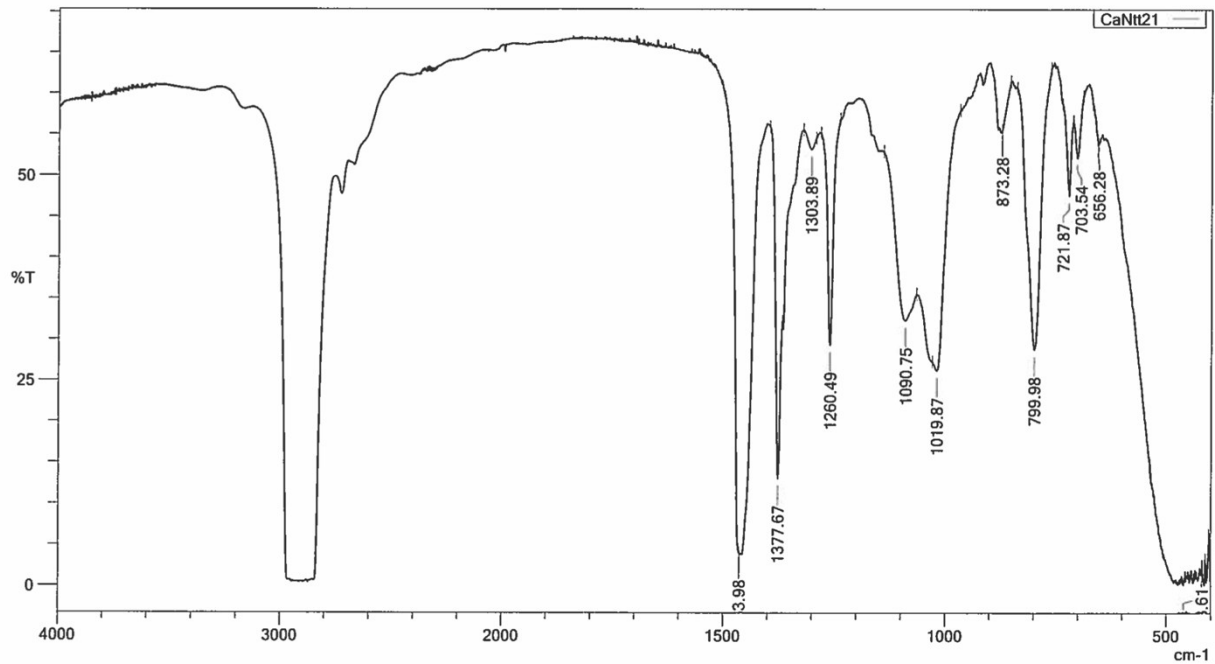
Figure S24. FTIR spectrum of **6** (Nujol mull, KBr discs).

4. X-ray Crystallography crystallographic data for 1-THF and 2-6

Crystal data for complexes **1-THF** and **2-6** are given in Tables S1-S2. Crystals were examined variously on an Oxford Diffraction Supernova diffractometer with a CCD area detector and a mirror-monochromated Mo Kα radiation (λ = 0.71073 Å) (**1-THF**, **2-3**, **5** and **6**), or a Bruker Apex II diffractometer with a CCD area detector and a graphite-monochromated Cu Kα radiation (λ = 1.54178 Å) (**4**). A Gaussian grid face-indexed absorption correction with a beam profile correction was applied. The structures were solved variously by direct and heavy atom methods and were refined by full-matrix least-squares on all unique F^2 values, with anisotropic displacement parameters for all non-hydrogen atoms, and with constrained riding hydrogen geometries. CrysAlisPro[2] was used for control and integration, and SHELXTL[3] and OLEX[4] were employed for structure solution. ORTEP-3[5] and POVRAY[6] was used for molecular graphics.

Table S5. Crystal data for **1-THF**, **2** and **3**.

^{a}Conventional $R = \Sigma||F_o| - |F_c||/\Sigma|F_o|$; $R_w = [\Sigma w(F_o^2 - F_c^2)^2/\Sigma w(F_o^2)^2]^{1/2}$; $S = [\Sigma w(F_o^2 - F_c^2)^2/\text{no. data} - \text{no.}$

params)]$^{1/2}$ for all data.

	1-THF	2	3
Formula	$C_{48}H_{54}KNO_3Si_2$	$C_{28}H_{68}MgN_2OSi_4$	$C_{30}H_{72}MgN_2Si_4$
Fw	788.20	585.51	597.56
cryst size, mm	0.15 x 0.17 x 0.44	0.13 x 0.27 x 0.36	0.36 x 0.40 x 0.45
crystal syst	triclinic	Triclinic	triclinic
space group	$P{-}1$	$P{-}1$	$P{-}1$
a, Å	11.7633(8)	10.0810(5)	12.0018(5)
b, Å	12.7083(7)	14.7993(8)	17.3410(7)
c, Å	17.4748(11)	15.5138(8)	20.7079(8)
α, °	70.553(5)	115.021(5)	68.970(4)
β, °	75.294(6)	90.373(4)	80.840(3)
γ, °	62.990(7)	93.593(4)	73.015(4)
V, Å^3	2178.2(3)	2091.8(2)	3840.1(3)
Z	2	2	4
ρ_{calcd}, g cm^3	1.202	0.930	1.034
μ, mm^{-1}	0.218	0.176	0.191
$F(000)$	840	652	1336
no. of reflections (unique)	7938	7652	14047
S^a	1.03	1.03	1.03
$R_1(wR_2)$ ($F^2 > 2\sigma(F^2)$)	0.0576 (0.1470)	0.0419 (0.1014)	0.0509 (0.1226)
R_{int}	0.023	0.027	0.042
min./max. diff map, Å^{-3}	−0.46, 0.61	−0.21, 0.25	−0.26, 0.32

Table S6. Crystal data for **4**, **5** and **6**.

[a]Conventional $R = \Sigma||F_o| - |F_c||/\Sigma|F_o|$; $R_w = [\Sigma w(F_o^2 - F_c^2)^2/\Sigma w(F_o^2)^2]^{1/2}$; $S = [\Sigma w(F_o^2 - F_c^2)^2/\text{no. data} - \text{no.}$

params)]$^{1/2}$ for all data.

	4	5	6
Formula	$C_{72}H_{60}MgN_2Si_4$	$C_{20}H_{46}IMgNO_2Si_2$	$C_{36}H_{84}CaN_2Si_4$
Fw	1089.89	539.97	697.49
cryst size, mm	0.10 x 0.10 x 0.20	0.08 x 0.10 x 0.16	0.26 x 0.30 x 0.37
crystal syst	tetragonal	Orthorhombic	orthorhombic
space group	$P–42_1c$	$Pbca$	$Pbca$
a, Å	13.9967(4)	19.3956(6)	20.5592(5)
b, Å	13.9967(4)	7.8668(2)	16.2479(7)
c, Å	14.5303(6)	6.2303(14)	26.1021(8)
α, °	90	90	90
β, °	90	90	90
γ, °	90	90	90
V, Å^3	2846.6(2)	5528.1(3)	8719.3(5)
Z	2	8	8
ρ_{calcd}, g cm^3	1.272	1.298	1.063
μ, mm^{-1}	1.430	1.282	0.279
$F(000)$	1148	2256	3120
no. of reflections (unique)	2604	5051	7967
S^a	1.06	1.04	1.01
$R_1(wR_2)$ ($F^2 > 2\sigma(F^2)$)	0.0293 (0.0770)	0.0381 (0.0820)	0.0589 (0.1383)
R_{int}	0.049	0.051	0.095
min./max. diff map, Å^{-3}	–0.22, 0.21	–0.53, 0.75	–0.28, 0.34

5. References

1. (a) R. Evans, G. D. Poggetto, M. Nillson and G. A. Morris, *Anal. Chem.*, 2018, **90**, 3987; (b) R. Evans, Z. Deng, A. K. Rogerson, A. S. McLachlan, J. J. Richards, M. Nilsson and G. A. Morris, *Angew. Chem. Int. Ed.*, 2013, **52**, 3199; (c) D. Li, I. Keresztes, R. Hopson and P. G. Willard, *Acc. Chem. Res.*, 2009, **42**, 270.

2. Agilent Technologies: Yarnton, England, 2010.

3. G. Sheldrick, *Acta Cryst.*, 2008, **A64**, 112.

4. O. V. Dolomanov, L. J. Bourhis, R. J. Gildea, J. A. K. Howard and H. Puschmann, *J. Appl. Cryst.*, 2009, **42**, 339.

5. L. J. Farrugia, *J. Appl. Cryst.*, 2012, **45**, 849.

6. POV-Ray, Persistence of Vision Raytracer Pty. Ltd.: Williamstown, Australia, 2004.